Charm-Quark Contribution to $K_L \to \mu^+\mu^-$ at Next-to-Next-to-Leading Order

Martin Gorbahn[1] and Ulrich Haisch[2]

[1]*Institut für Theoretische Teilchenphysik, Universität Karlsruhe, D-76128 Karlsruhe, Germany*
[2]*Institut für Theoretische Physik, Universität Zürich, CH-8057 Zürich, Switzerland*

(Received 4 July 2006; published 21 September 2006)

We calculate the charm-quark contribution to the decay $K_L \to \mu^+\mu^-$ in next-to-next-to-leading order of QCD. This new contribution reduces the theoretical uncertainty in the relevant parameter P_c from $\pm 22\%$ down to $\pm 7\%$, corresponding to scale uncertainties of $\pm 3\%$ and $\pm 6\%$ in the short-distance part of the branching ratio and the determination of the Wolfenstein parameter $\bar{\rho}$ from $K_L \to \mu^+\mu^-$. The error in $P_c = 0.115 \pm 0.018$ is now in equal shares due to the combined scale uncertainties and the current uncertainty in the charm-quark mass. We find $\mathcal{B}(K_L \to \mu^+\mu^-)_{\rm SD} = (0.79 \pm 0.12) \times 10^{-9}$, with the present uncertainty in the Cabibbo-Kobayashi-Maskawa element V_{td} being the dominant individual source in the quoted error.

DOI: 10.1103/PhysRevLett.97.122002 PACS numbers: 12.38.Bx, 13.20.Eb

The study of the rare process $K_L \to \mu^+\mu^-$ has played a central role in unraveling the flavor content and structure of the standard model (SM) of electroweak interactions [1]. These glory days have passed, but still today $K_L \to \mu^+\mu^-$ provides useful information on the short-distance dynamics of $|\Delta S| = 1$ flavor-changing-neutral-current transitions despite the fact that its decay amplitude is dominated by the long-distance two-photon contribution $K_L \to \gamma^*\gamma^* \to \mu^+\mu^-$. While the absorptive part of the latter correction is calculable with high precision in terms of the $K_L \to \gamma\gamma$ rate the corresponding dispersive part represents a significant source of theoretical uncertainty. In fact long- and short-distance dispersive pieces cancel against each other in large parts and the measured total $K_L \to \mu^+\mu^-$ rate [2] is nearly saturated by the absorptive two-photon contribution. The precision in the determination of the dispersive pieces therefore controls the accuracy of possible bounds on the real part of the Cabibbo-Kobayashi-Maskawa (CKM) element V_{td} or, equivalently, the Wolfenstein parameter $\bar{\rho}$. In view of the recent experimental [3] and theoretical [4] developments concerning the dispersive long-distance part of the $K_L \to \mu^+\mu^-$ decay amplitude it is also worthwhile to improve the theoretical accuracy of the associated short-distance contribution. This is the purpose of this Letter.

The branching ratio for the dispersive short-distance part of $K_L \to \mu^+\mu^-$ can be written as [5]

$$\mathcal{B}(K_L \to \mu^+\mu^-)_{\rm SD} = \kappa_\mu \left[\frac{{\rm Re}\lambda_t}{\lambda^5} Y(x_t) + \frac{{\rm Re}\lambda_c}{\lambda} P_c \right]^2, \tag{1}$$

$$\kappa_\mu \equiv \frac{\alpha^2 \mathcal{B}(K^+ \to \mu^+\nu_\mu)}{\pi^2 \sin^4\theta_W} \frac{\tau(K_L)}{\tau(K^+)} \lambda^8 = (2.009 \pm 0.017) \times 10^{-9} \left(\frac{\lambda}{0.225} \right)^8, \tag{2}$$

where $\lambda_i \equiv V_{is}^* V_{id}$ denote the relevant CKM factors. There is also a short-distance two-loop electroweak contribution in the two-photon mediated decay amplitude [6]. Following [4], where this contribution is included in the two-photon correction itself, we do not add it to the short-distance contribution in Eq. (1). The apparent strong dependence of $\mathcal{B}(K_L \to \mu^+\mu^-)_{\rm SD}$ on $\lambda \equiv |V_{us}|$ is spurious as P_c is proportional to $1/\lambda^4$. In quoting the value for P_c we will set $\lambda = 0.225$. The electromagnetic coupling α and the weak mixing angle $\sin^2\theta_W$ entering $\mathcal{B}(K_L \to \mu^+\mu^-)$ are naturally evaluated at the electroweak scale [7]. Then the leading term in the heavy top expansion of the electroweak two-loop corrections to $Y(x_t)$ amounts to typically -1.5% for the modified minimal subtraction scheme ($\overline{\rm MS}$) definition of α and $\sin^2\theta_W$ [8]. In obtaining the numerical value of Eq. (2) we have employed $\alpha \equiv \alpha_{\overline{\rm MS}}(M_Z) = 1/127.9$, $\sin^2\theta_W \equiv \sin^2\hat{\theta}_W^{\overline{\rm MS}} = 0.231$, and $\mathcal{B}(K^+ \to \mu^+\nu_\mu) = (63.39 \pm 0.18) \times 10^{-2}$ [9].

The function $Y(x_t)$ in Eq. (1) depends on the top quark $\overline{\rm MS}$ mass through $x_t \equiv m_t^2(\mu_t)/M_W^2$. It originates from Z-penguin and electroweak box diagrams with an internal top quark. As the relevant operator has a vanishing anomalous dimension and the energy scales involved are of the order of the electroweak scale or higher, the function $Y(x_t)$ can be calculated within ordinary perturbation theory. It is known through next-to-leading order (NLO) [10,11], with a scale uncertainty due to the top quark matching scale $\mu_t = \mathcal{O}(m_t)$ of slightly more than $\pm 2\%$. Converting the top quark pole mass of $M_t = (172.5 \pm 2.3)$ GeV [12] at three loops to $m_t(M_t)$ [13] and relating $m_t(M_t)$ to $m_t(m_t) = (162.8 \pm 2.2)$ GeV using the one-loop renormalization group (RG), we find $Y(x_t) = 0.950 \pm 0.049$. The given uncertainty combines linearly an error of ± 0.029 due to the error of $m_t(m_t)$ and an error of ± 0.020 obtained by varying μ_t in the range 60 GeV $\leq \mu_t \leq$ 240 GeV.

The calculable parameter P_c entering Eq. (1) results from Z-penguin and electroweak box diagrams involving internal charm-quark exchange. As now both high- and

low-energy scales, namely, $\mu_W = \mathcal{O}(M_W)$ and $\mu_c = \mathcal{O}(m_c)$, are involved, a complete RG analysis of this term is required. In this manner, large logarithms $\ln(\mu_W^2/\mu_c^2)$ are resummed to all orders in α_s. The large scale uncertainty due to μ_c of $\pm 44\%$ in the leading order result was a strong motivation for the NLO analysis of this contribution [5,11].

Performing the RG running from μ_W down to $\mu_b = \mathcal{O}(m_b)$ in an effective five-flavor theory and the subsequent evolution from μ_b down to μ_c in an effective four-flavor theory, we obtain at NLO

$$P_c = 0.106 \pm 0.023_{\text{theor}} \pm 0.009_{m_c} \pm 0.001_{\alpha_s} = (0.106 \pm 0.034)\left(\frac{0.225}{\lambda}\right)^4, \quad (3)$$

where the parametric errors correspond to the ranges of the charm-quark $\overline{\text{MS}}$ mass $m_c(m_c)$ and the strong coupling constant $\alpha_s(M_Z)$ given in Table I. The final error has been obtained by performing a detailed analysis of the individual sources of uncertainty entering the NLO prediction of P_c using a modified version of the CKMFITTER package [15]. The same statistical treatment of errors will be applied in Eqs. (4), (8), and (9).

The dependence of P_c on μ_c can be seen in Fig. 1. The solid line in the upper plot shows the NLO result obtained by evaluating $\alpha_s(\mu_c)$ from $\alpha_s(M_Z)$ solving the RG equation of α_s numerically, while the dashed and dotted lines are obtained by first determining the scale parameter $\Lambda_{\overline{\text{MS}}}$ from $\alpha_s(M_Z)$, either using the explicit solution of the RG equation of α_s or by solving the RG equation of α_s iteratively for $\Lambda_{\overline{\text{MS}}}$, and subsequently calculating $\alpha_s(\mu_c)$ from $\Lambda_{\overline{\text{MS}}}$. The corresponding two-loop values for $\alpha_s(\mu_c)$ have been obtained with the program RUNDEC [16]. Obviously, the difference between the three curves is due to higher order terms and has to be regarded as part of the theoretical error. With its size of ± 0.006 it is almost comparable to the variation of the NLO result due to μ_c, amounting to ± 0.016. In [5] a larger value for the latter uncertainty has been quoted. The observed difference is related to the definition of the charm-quark mass. Replacing $m_c(m_c)$ in the logarithms $\ln(\mu_c^2/m_c^2)$ of the one-loop matrix elements by the more appropriate $m_c(\mu_c)$ leads to a significant reduction of the dependence of P_c on μ_c. A detailed discussion of this issue can be found in [17]. Finally, while in [5] only μ_c was varied, the theoretical error given in Eq. (3) includes also the dependence on μ_b and μ_W of combined ± 0.001. The specified scale uncertainties correspond to the ranges $1\ \text{GeV} \le \mu_c \le 3\ \text{GeV}$, $2.5\ \text{GeV} \le \mu_b \le 10\ \text{GeV}$, and $40\ \text{GeV} \le \mu_W \le 160\ \text{GeV}$.

TABLE I. Input parameters used in the numerical analysis of P_c, $\mathcal{B}(K_L \to \mu^+\mu^-)_{\text{SD}}$ and $\bar{\rho}$.

Parameter	Value $\pm$ Error	Reference
$m_c(m_c)$ [GeV]	1.30 ± 0.05	[14], our average
$\alpha_s(M_Z)$	0.1187 ± 0.0020	[9]
$\text{Re}\lambda_t$ $[10^{-4}]$	$-3.11^{+0.13}_{-0.14}$	[15]
$\text{Re}\lambda_c$	$-0.22098^{+0.00095}_{-0.00091}$	[15]

Using the input parameters listed in Table I, we find from Eqs. (1)–(3) at NLO

$$\mathcal{B}(K_L \to \mu^+\mu^-)_{\text{SD}} = (0.77 \pm 0.08_{P_c} \pm 0.08_{\text{other}}) \times 10^{-9} = (0.77 \pm 0.16) \times 10^{-9}, \quad (4)$$

where the second error in the first line collects the uncertainties due to κ_μ, $Y(x_t)$ and the CKM elements.

As the uncertainties in Eqs. (3) and (4) coming from M_t, $m_c(m_c)$ and the CKM parameters should be decreased in the coming years it is also desirable to reduce the theoretical uncertainty in P_c. To this end, we here extend the NLO analysis of P_c presented in [5,11] to the next-to-next-to-leading order (NNLO). This requires the computation of three-loop anomalous dimensions of certain operators and of certain two-loop contributions.

The main components of the NNLO calculation, which aims at resumming all $\mathcal{O}(\alpha_s^n \ln^{n-1}(\mu_W^2/\mu_c^2))$ logarithms in P_c, are (i) the $\mathcal{O}(\alpha_s^2)$ matching corrections to the relevant Wilson coefficients arising at μ_W, (ii) the $\mathcal{O}(\alpha_s^3)$ anomalous dimensions describing the mixing of the dimension-six and -eight operators, (iii) the $\mathcal{O}(\alpha_s^2)$ threshold correc-

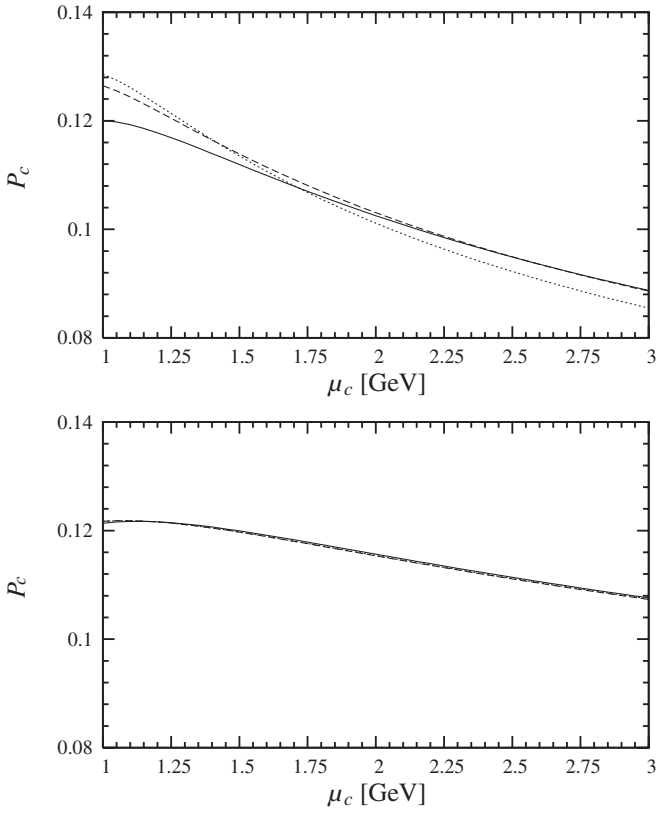

FIG. 1. P_c as a function of μ_c at NLO (upper plot) and NNLO (lower plot). The three different lines correspond to three different methods of computing $\alpha_s(\mu_c)$ from $\alpha_s(M_z)$ (see text).

tions to the Wilson coefficients originating at μ_b, and (iv) the $\mathcal{O}(\alpha_s^2)$ matrix elements of some of the operators emerging at μ_c. To determine the contributions of type (i), (iii), and (iv) one must calculate two-loop Green functions in the full SM and in effective theories with five or four flavors. Sample diagrams for steps (i) and (iv) are shown in the left and right columns of Fig. 2. The contributions (ii) are found by calculating three-loop Green functions with operator insertions. Sample diagrams with a double insertion of dimension-six operators are shown in the center column of Fig. 2.

The Z-penguin contribution can be trivially obtained from that in $K^+ \to \pi^+ \nu\bar{\nu}$, which has been recently computed at NNLO [17,18]. The electroweak box contribution on the other hand is slightly different for $K_L \to \mu^+\mu^-$ and $K^+ \to \pi^+ \nu\bar{\nu}$, since the lepton line in the corresponding Feynman diagrams is reversed and thus requires a new calculation. A comprehensive discussion of the technical details of the matching and the renormalization of the effective theory can be found in [17].

In the following we present only the final result for the $\mathcal{O}(\alpha_s^2)$ matching correction $C_\mu^{B(2)}$, the $\mathcal{O}(\alpha_s^3)$ anomalous dimension $\gamma_\mu^{B(2)}$, and the $\mathcal{O}(\alpha_s^2)$ matrix element $r_\mu^{B(2)}$. Employing the operator basis of [5,11] we obtain for the standard choices of Casimir operators $C_A = 3$, $C_F = 4/3$, and f active quark flavors

$$
\begin{aligned}
C_\mu^{B(2)} &= \frac{416}{3} + \frac{16\pi^2}{3} + \frac{272}{3}\ln\frac{\mu_W^2}{M_W^2} + 16\ln^2\frac{\mu_W^2}{M_W^2},\\
\gamma_\mu^{B(2)} &= \frac{27\,032}{9} - 1088\zeta(3) - \frac{1040}{9}f,\\
r_\mu^{B(2)} &= -\frac{112}{3} - \frac{80}{3}\ln\frac{\mu_c^2}{m_c^2} - 16\ln^2\frac{\mu_c^2}{m_c^2}.
\end{aligned}
\tag{5}
$$

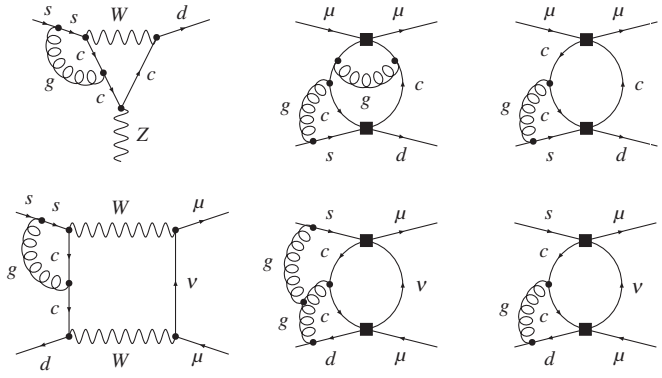

FIG. 2. Examples of Feynman diagrams arising in the full SM (left column), describing the mixing of operators (center column) and the matrix elements (right column) in the Z-penguin (upper row) and the electroweak box (lower row) sector. Only the divergent pieces of the diagrams displayed in the center column have to be computed, while the Feynman graphs shown on the left- and right-hand side are needed including their finite parts.

Here $\zeta(x)$ is the Riemann zeta function with the value $\zeta(3) \approx 1.20\,206$ and $m_c \equiv m_c(\mu_c)$ denotes the charm-quark $\overline{\text{MS}}$ mass. Our results for the NLO Wilson coefficient, the anomalous dimension and the matrix element agree with the findings of [11] where an error made in the original calculation [5] has been corrected.

The analytic expression for P_c including the complete NNLO corrections is too complicated and too long to be presented here. Instead setting $\lambda = 0.225$, $m_t(m_t) = 162.8$ GeV and $\mu_W = 80.0$ GeV we derive an approximate formula for P_c that summarizes the dominant parametric and theoretical uncertainties due to $m_c(m_c)$, $\alpha_s(M_Z)$, μ_c, and μ_b. It reads

$$
\begin{aligned}
P_c = 0.1198&\left(\frac{m_c(m_c)}{1.30\ \text{GeV}}\right)^{2.3595}\left(\frac{\alpha_s(M_Z)}{0.1187}\right)^{6.6055}\\
&\times\left(1 + \sum_{i,j,k,l}\kappa_{ijlm} L_{m_c}^i L_{\alpha_s}^j L_{\mu_c}^k L_{\mu_b}^l\right),
\end{aligned}
\tag{6}
$$

where

$$
\begin{aligned}
L_{m_c} &= \ln\left(\frac{m_c(m_c)}{1.30\ \text{GeV}}\right), \qquad L_{\alpha_s} = \ln\left(\frac{\alpha_s(M_Z)}{0.1187}\right),\\
L_{\mu_c} &= \ln\left(\frac{\mu_c}{1.5\ \text{GeV}}\right), \qquad L_{\mu_b} = \ln\left(\frac{\mu_b}{5.0\ \text{GeV}}\right),
\end{aligned}
\tag{7}
$$

and the sum includes the expansion coefficients κ_{ijkl} given in Table II. The above formula approximates the exact NNLO result with an accuracy of better than $\pm 1.0\%$ in the ranges $1.15\ \text{GeV} \le m_c(m_c) \le 1.45\ \text{GeV}$, $0.1150 \le \alpha_s(M_Z) \le 0.1230$, $1.0\ \text{GeV} \le \mu_c \le 3.0\ \text{GeV}$, and $2.5\ \text{GeV} \le \mu_b \le 10.0\ \text{GeV}$. The uncertainties due to $m_t(m_t)$, μ_W and the different methods of computing $\alpha_s(\mu_c)$ from $\alpha_s(M_Z)$, which are not quantified above, are all below $\pm 0.2\%$. Their actual size at NNLO will be discussed below.

Using the input parameters listed in Table I, we find at the NNLO level

$$
\begin{aligned}
P_c &= 0.115 \pm 0.008_{\text{theor}} \pm 0.008_{m_c} \pm 0.001_{\alpha_s}\\
&= (0.115 \pm 0.018)\left(\frac{0.225}{\lambda}\right)^4,
\end{aligned}
\tag{8}
$$

where now the residual scale ambiguities and the uncertainty due to $m_c(m_c)$ are of the same size. Comparing these numbers with Eq. (3) we observe that our NNLO calculation reduces the theoretical uncertainty by a factor of more than 3.

TABLE II. The coefficients κ_{ijkl} arising in the approximate formula for P_c at NNLO.

$\kappa_{1000} = -0.5373$	$\kappa_{0100} = -6.0472$	$\kappa_{0010} = -0.0956$
$\kappa_{0001} = 0.0114$	$\kappa_{1100} = 3.9957$	$\kappa_{1010} = 0.3604$
$\kappa_{0110} = 0.0516$	$\kappa_{0101} = -0.0658$	$\kappa_{2000} = -0.1767$
$\kappa_{0200} = 16.4465$	$\kappa_{0020} = -0.1294$	$\kappa_{0030} = 0.0725$

As can be nicely seen in the lower plot of Fig. 1, P_c depends very weakly on μ_c at NNLO, varying by only ± 0.007. Furthermore, the three different treatments of α_s affect the NNLO result in a negligible way. The three-loop values of $\alpha_s(\mu_c)$ used in the numerical analysis have been obtained with the program RUNDEC. The theoretical error quoted in Eq. (8) includes also the dependence on μ_b and μ_W of combined ± 0.001. The presented scale uncertainties correspond to the ranges given earlier.

Using Eqs. (1), (2), and (8) the result in Eq. (4) is modified to the NNLO value

$$\mathcal{B}(K_L \to \mu^+\mu^-)_{\mathrm{SD}} = (0.79 \pm 0.04_{P_c} \pm 0.08_{\mathrm{other}}) \times 10^{-9} = (0.79 \pm 0.12) \times 10^{-9}. \quad (9)$$

Obviously, at present the errors from M_t, $m_c(m_c)$ and the CKM parameters veil the benefit of the NNLO calculation of P_c presented in this Letter.

Provided both P_c and $\mathcal{B}(K_L \to \mu^+\mu^-)_{\mathrm{SD}}$ are known with sufficient precision useful bounds on the Wolfenstein parameter $\bar{\rho}$ can be obtained [5]. In particular for the measured branching ratio $\mathcal{B}(K_L \to \mu^+\mu^-)_{\mathrm{SD}}$ close to its SM predictions, one finds that given uncertainties $\sigma(P_c)$ and $\sigma(\mathcal{B}(K_L \to \mu^+\mu^-)_{\mathrm{SD}})$ translate into

$$\frac{\sigma(\bar{\rho})}{\bar{\rho}} = \pm 0.89 \frac{\sigma(P_c)}{P_c} \pm 2.59 \frac{\sigma(\mathcal{B}(K_L \to \mu^+\mu^-)_{\mathrm{SD}})}{\mathcal{B}(K_L \to \mu^+\mu^-)_{\mathrm{SD}}}. \quad (10)$$

As seen in Eq. (10) the accuracy of the determination of $\bar{\rho}$ depends sensitively on the error in P_c. The reduction of the theoretical error in P_c from $\pm 22\%$ down to $\pm 7\%$ translates into the following uncertainties

$$\frac{\sigma(\bar{\rho})}{\bar{\rho}} = \begin{cases} \pm 20\%, & \text{NLO}, \\ \pm 6\%, & \text{NNLO}, \end{cases} \quad (11)$$

implying a significant improvement of the NNLO over the NLO result. In obtaining these numbers we have included only the theoretical errors quoted in Eqs. (3) and (8).

Using the conservative upper bound

$$\mathcal{B}(K_L \to \mu^+\mu^-)_{\mathrm{SD}} < 2.5 \times 10^{-9}, \quad (12)$$

on the short-distance part of the $K_L \to \mu^+\mu^-$ branching ratio derived in [4], we find the following allowed range

$$-0.74 < \bar{\rho} < 3.13, \quad (13)$$

for the Wolfenstein parameter $\bar{\rho}$ employing a customized version of the CKMFITTER code.

To conclude, we have evaluated the complete NNLO correction of the charm-quark contribution to $\mathcal{B}(K_L \to \mu^+\mu^-)_{\mathrm{SD}}$. The inclusion of these contributions leads to a drastic reduction of the theoretical uncertainty in the relevant parameter P_c. This strengthens the power of the rare decay $K_L \to \mu^+\mu^-$ in determining the Wolfenstein parameter $\bar{\rho}$ from its short-distance branching ratio.

We would like to thank A. J. Buras and U. Nierste for carefully reading the manuscript, A. Höcker and J. Ocariz for useful correspondence concerning the CKMFITTER package, and I. Picek and S. Trine for informative communications regarding the two-loop electroweak two-photon contribution. U. H. has been supported by the Schweizer Nationalfonds.

[1] S. L. Glashow, J. Iliopoulos, and L. Maiani, Phys. Rev. D **2**, 1285 (1970); M. K. Gaillard and B. W. Lee, Phys. Rev. D **10**, 897 (1974).
[2] D. Ambrose *et al.* (E871 Collaboration), Phys. Rev. Lett. **84**, 1389 (2000).
[3] A. Alavi-Harati *et al.* (KTeV Collaboration), Phys. Rev. Lett. **87**, 071801 (2001); **90**, 141801 (2003).
[4] G. Isidori and R. Unterdorfer, J. High Energy Phys. 01 (2004) 009 and references therein.
[5] G. Buchalla and A. J. Buras, Nucl. Phys. **B412**, 106 (1994).
[6] J. O. Eeg, K. Kumericki and I. Picek, Eur. Phys. J. C **1**, 531 (1998).
[7] C. Bobeth *et al.*, J. High Energy Phys. 04 (2004) 071.
[8] G. Buchalla and A. J. Buras, Phys. Rev. D **57**, 216 (1998).
[9] S. Eidelman *et al.* (Particle Data Group), Phys. Lett. B **592**, 1 (2004); 2005 partial update for edition 2006 available at http://pdg.lbl.gov/.
[10] G. Buchalla and A. J. Buras, Nucl. Phys. **B398**, 285 (1993); **B400**, 225 (1993); M. Misiak and J. Urban, Phys. Lett. B **451**, 161 (1999).
[11] G. Buchalla and A. J. Buras, Nucl. Phys. **B548**, 309 (1999).
[12] E. Brubaker *et al.* (Tevatron Electroweak Working Group), hep-ex/0603039.
[13] K. G. Chetyrkin and M. Steinhauser, Phys. Rev. Lett. **83**, 4001 (1999); Nucl. Phys. **B573B**, 617 (2000); K. Melnikov and T. v. Ritbergen, Phys. Lett. B **482**, 99 (2000).
[14] J. H. Kühn and M. Steinhauser, Nucl. Phys. **B619**, 588 (2001); **B640**, 415(E) (2002); J. Rolf and S. Sint (ALPHA Collaboration), J. High Energy Phys. 12 (2002) 007; A. H. Hoang and M. Jamin, Phys. Lett. B **594**, 127 (2004); O. Buchmüller and H. Flächer, Phys. Rev. D **73**, 073008 (2006); A. H. Hoang and A. V. Manohar, Phys. Lett. B **633**, 526 (2006); K. G. Chetyrkin, J. H. Kühn, and C. Sturm, hep-ph/0604234; R. Boughezal, M. Czakon, and T. Schutzmeier, hep-ph/0605023.
[15] J. Charles *et al.* (CKMfitter Group), Eur. Phys. J. C **41**, 1 (2005), updated results available at http://ckmfitter.in2p3.fr.
[16] K. G. Chetyrkin, J. H. Kühn, and M. Steinhauser, Comput. Phys. Commun. **133**, 43 (2000).
[17] A. J. Buras *et al.*, hep-ph/0603079.
[18] A. J. Buras *et al.*, Phys. Rev. Lett. **95**, 261805 (2005).